

# Automated Detection of Branch Dimensions in Woody Skeletons of Fruit Tree Canopies

Alexander Bucksch and Stefan Fleck

## Abstract

*Modeling the 3D canopy structure of trees provides the structural mapping capability on which to assign distributed values of light-driven physiological processes in tree canopies. We evaluate the potential of automatically extracted skeletons from terrestrial lidar data as a basis for modeling canopy structure. The automatic and species independent evaluation method for lidar data of trees is based on the SKELTRE algorithm. The SKELTRE skeleton is a graphical representation of the branch hierarchy. The extraction of the branch hierarchy utilizes a graph splitting procedure to extract the branches from the skeleton. Analyzing the distance between the point cloud points and the skeleton is the key to the branch diameter. Frequency distributions of branch length and diameter were chosen to test the algorithm performance in comparison to manually measured data and resulted in a correlation of up to 0.78 for the branch length and up to 0.99 for the branch diameter.*

## Introduction

Branch systems of trees are the result of ramification and branch elongation processes that occur, outside the tropics, in an annual rhythm. The pattern of branch elongation and radial diameter growth can reveal the dendritic growth history of trees with the same accuracy as growth-ring chronologies of the trunk (Roloff, 1986). The annual rhythm of growth conditions is reflected in the branching pattern of trees and will finally be represented in the skeleton. Furthermore, the dendrochronological patterns are closely correlated to other structural quantities of tree canopies like appending leaf or woody biomass (Niklas, 1994). Allometric equations were established on this basis for many tree species in order to derive the amount of woody biomass (Bartelink, 1997), leaf biomass (Burger, 1945) or distribution of leaf biomass in space (Fleck, 2002) from more easily measured features such as trunk or branch diameters. 3D-canopy light modeling depends on such spatial information as the distribution of biomass and is the key to a number of physiological processes in the canopy that express the vitality and performance of trees (Fleck *et al.*, 2004).

---

Alexander Bucksch is at the Delft Institute of Earth Observation and Space Systems (DEOS), Delft University of Technology, Kluyverweg 1, 2629 HS Delft, The Netherlands, (a.k.bucksch@tudelft.nl).

Stefan Fleck is with the Department Environmental Control, North-West German Forest Research Institute, Graetzelstrasse 2, 37079 Göttingen, Germany, and formerly with Plant Ecology, Albrecht-von-Haller-Institute of Plant Sciences, University of Göttingen, Untere Karspüle 2, 37073 Göttingen, Germany.

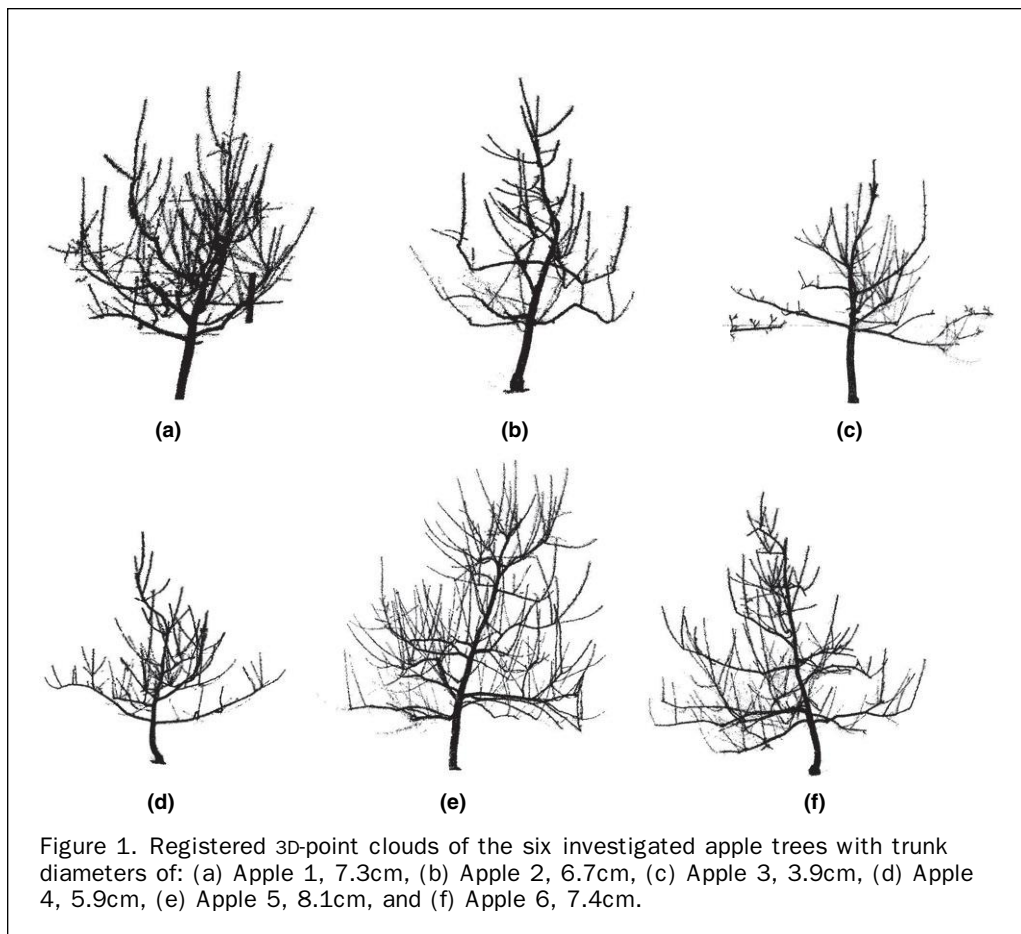
From a remote sensing viewpoint, the automated assessment of branch dimensions in the canopy is unprecedented. Terrestrial laser scanners measure thousands of distances per second between the instrument and its surroundings at regular horizontal and vertical angles (Shan and Toth, 2008) in order to represent a high-resolution 3D point cloud. Thus, terrestrial lidar enables the measurement of the complete three-dimensional structure of the branching system. This branching information can be made available to modelers in biology and forestry. An automated evaluation procedure would make it possible to overcome tedious measurement procedures or inaccurate estimations of the branching system.

In one sense, laser scanning produces a discrete surface sampling of a real world object and represents it as a point cloud. Single scans must be made from different scanning positions to render the whole object. The scans have to then be co-located into one common coordinate system. The process of aligning scans into a common coordinate system is called registration. The drawback of the registration procedure is that regularity in the scan data vanishes, and the point cloud becomes unorganized. Furthermore, the height distribution of the reference points to perform the registration is critical (Henning and Radtke, 2006) and influences the registration result. The study of unorganized point clouds as an object representation and the possible information to be extracted from point clouds is an area of active research. Although the majority of research has focused on the extraction of surface parameters from the point cloud, e.g., Pfeifer *et al.* (2004) and Henning and Radtke (2008), this paper describes a new method to reveal the branching information using the example of leafless apple trees. The fully automatic approach presented here does not depend on species information, such as allometric relationships. Obtaining the branching system from unorganized point clouds (Figure 1) can help in various point cloud applications. The target application of this paper is the extraction of the branch length and diameter from laser-scanned orchard trees. The SKELTRE-skeleton used in this research represents the tree's branching system as a graph. Such a graph consists of vertices which are connected by edges. Every vertex corresponds to a distinct part of the point cloud and is embedded into the centre of the corresponding point cloud part. The edges are assumed as straight connections between the embedded vertices. The skeleton extraction from a point cloud faces several algorithmic challenges, such as centeredness, topological

---

Photogrammetric Engineering & Remote Sensing  
Vol. 77, No. 3, March 2011, pp. 229–240.

0099-1112/11/7703-0229/\$3.00/0  
© 2011 American Society for Photogrammetry  
and Remote Sensing



correctness, and robustness to noise. These challenges are described in more detail in Bucksch *et al.* (2009a) and Bucksch *et al.* (2010).

#### Review of Tree Skeletonization from Laser Scanned Point Clouds

Literature on skeletonization of trees from real data like laser scans is limited, although skeletonization is a heavily studied topic in theory. For general information about skeletal structures, the reader is referred to Biasotti *et al.* (2007), while the review given here is related to tree skeletonization as a special case.

Gorte *et al.* (2004) presented a first approach to tree skeletonization using mathematical morphology. Their algorithm used the sequential data thinning method of Palágyi *et al.* (2001) and applied it to terrestrial laser scan data. The morphological operations of opening and erosion were used to produce a skeleton (Serra, 1982) and applied to a rasterized point cloud, in which every raster cell contained several measuring points. One drawback of this algorithm is the large number of parameters that need to be controlled, such as the resolution of the raster and the type and size of the structuring element. From a theoretical perspective, centering within the point cloud is difficult and connectivity cannot be guaranteed. This approach was later extended to the so-called Dijkstra skeletonization (Gorte, 2006). The connectivity of the skeleton was improved by comparing different raster resolutions. The major common drawback is that the extraction of a centerline from an object like a tree requires a completely represented object hull in order to fill the inner volume with raster cells. Occlusion effects often make this difficult to achieve with trees.

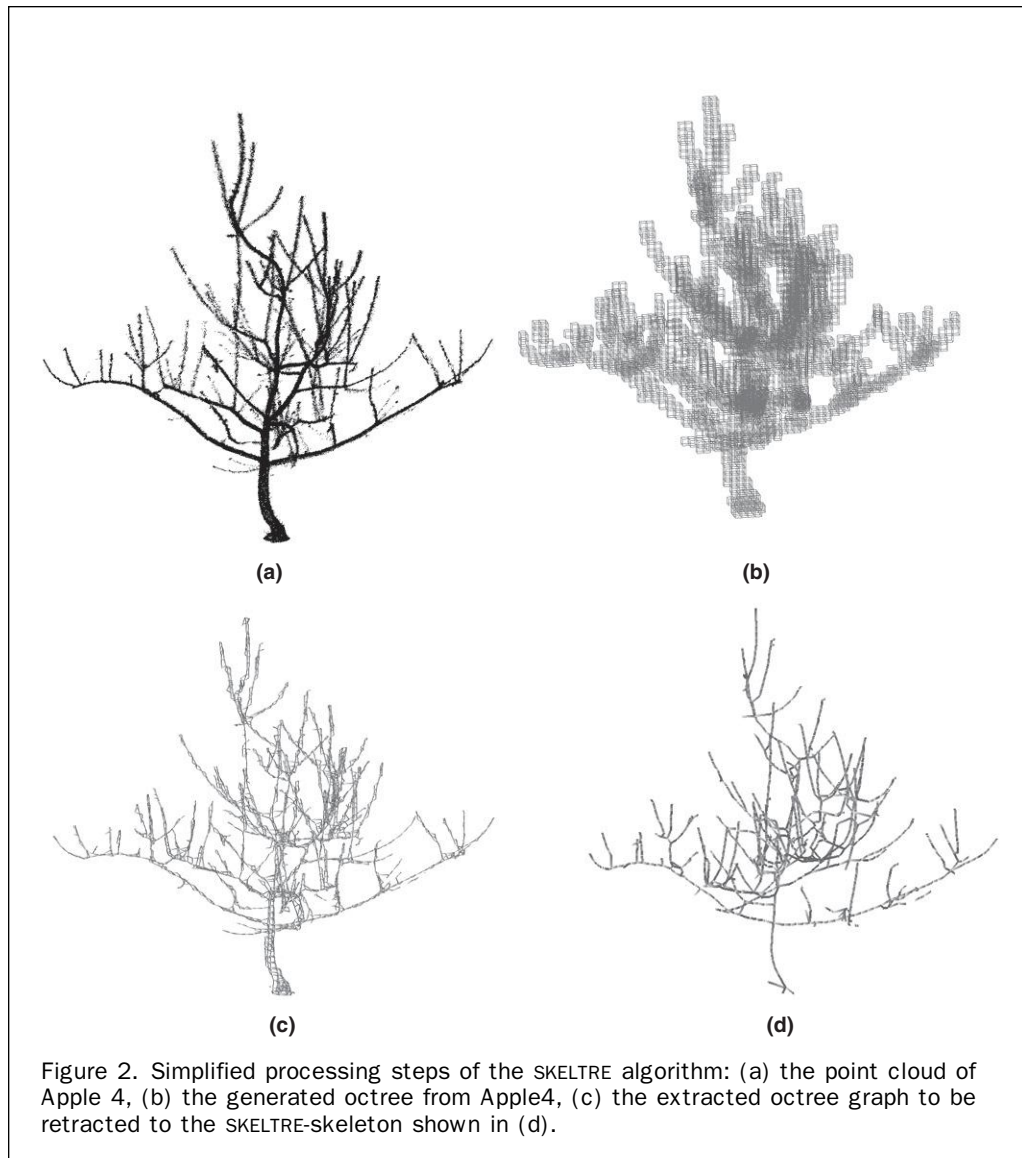
Bucksch *et al.* (2008) used an adaptive octree to subdivide the point cloud. Their octree subdivision relied on the directions in which the point cloud passes through the octree cell sides. This is the key to operate on only a few data points if necessary. The algorithm requires only one input parameter, which is the minimum allowable cell size to terminate the subdivision process. From this octree, an initial graph, the so-called octree graph, is extracted (Figure 2c). This octree graph is reduced to the SKELTRESkeleton (Figure 2d). The reduction follows a set of rules, which are applied to redundant structures in the graph.

Recently a semi-automatic approach using tree allometries to produce a model of a tree designed for visualization purposes was introduced by Xu *et al.* (2007). The described procedure computes a rough skeleton of the main branches up to approximately 66 percent of the tree height. The remaining tree is generated based on prior knowledge and creates a plausible model for visualization. A similar approach was introduced by Yan *et al.* (2009). They used a clustering method to extract the skeleton from a laser scanned tree without leaves. Yan *et al.* (2009) compared their results qualitatively to Xu *et al.* (2007) based on examples. They concluded that their clustering algorithm represents the branching system better than the approach of Xu *et al.* (2007).

## Methods

### Study Area

The study was mainly conducted in apple orchards of the Annapolis Valley, Nova Scotia, Canada close to the city of



Kentville (45°4'39"N, 64°29'45"W). The six investigated apple trees (*Malus x domestica* Borkh.: "Honeycrisp") were located in two orchards that belong to the test sites of the Atlantic Food and Horticulture Research Centre (Fleck *et al.*, 2010a). Three apple trees grew on a trellis system, and the other three trees stood as single trees in rows. The orientation of the rows is from North to South with a tree spacing of 3 m within each row and a spacing of 5 m between rows. Trees of comparable height were located next to the investigated trees. The manually-measured trunk diameters ranged from 3.9 cm to 8.1 cm. The tree height of the six apple trees varied from 1.27 m to 3.03 m.

#### Field Measurements

Each tree was scanned in March 2006 with the 3D-laserscanner Imager 5003 (Zoller+Fröhlich, Germany) from four sides (approximately North-East, South-East, South-West, North-West) at a distance of about 4 m to the trunk. The laser scanner was placed at different heights above the ground (between 1 m and 2.3 m) in order to maximize coverage of the measured tree surface. The scanner resolution was set to "High" which is equal to a horizontal and vertical angular step width of 0.036 degrees and results in a 10,000 pixel

resolution for 360 degrees. A branch of the tree was identified as elongated woody element with a minimum diameter of 3 mm, inserting at a ramification point (node) on another, usually a thicker branch or trunk element. The branches of each tree were numbered for reconstructing the branch hierarchy, and their length was measured following the elongation direction of the branch. The diameter of each branch was measured at its base and tip, about 1 cm before the node or end bud. The diameters of branches were measured with a caliper in two directions and averaged. If both diameter measurements were more than 1 mm apart, a third diameter measurement was taken and the average of three measurements was taken. Branch diameters thicker than 5 cm were derived from circumference measurements with a meter tape assuming the trunk or main branch to have a circular cross-section.

#### Data Processing

Registration of the scans was done with the NEPTAN-based registration algorithm in Z+F Laser Control based on 14 to 18 artificial targets that were placed on the ground and fixed to ladders at a height of about 2 m in order to achieve a homogeneous distribution of tie points common to multiple

scans. The 3D-point cloud was transferred to the software Cyclone (Leica Geosystems) and subsamples representing a single tree were isolated (Fleck *et al.*, 2007). Skeletonization of each 3D-point cloud was performed with the SKELTRE algorithm (Bucksch *et al.*, 2009a), an algorithm used to extract a skeleton from the unorganized point clouds of the trees. The space occupied by the tree point cloud (Figure 2a) is subdivided by an octree. An octree subdivides the space into cubic cells (Figure 2b).

From these octree cells, a graph is extracted. The graph extraction is based on an estimate of how the actual surface represented by the point cloud crosses the octree cell sides. The edges of the SkelTre-skeleton indicate the crossing direction through the octree cells. Every edge belongs to two vertices and is associated with a directional edge label. The edge labels produced by the algorithm, guarantee that the initially extracted graph is reduced to a one-dimensional skeleton by merging neighboring vertices. Neighboring vertices are defined to be connected by an edge. In order to decide which neighboring vertices are merged, a set of rules is used to assure that the branching of the tree corresponds to the branching of the skeleton, Bucksch *et al.* (2009a) and Bucksch *et al.* (2010). One benefit of the SKELTRE skeleton is that the centeredness of the vertices corresponds to a unique point cloud part. Here centeredness is the center of gravity of all points belonging to a vertex. Another benefit is that the extracted branching hierarchy is embedded into a well-known topological framework (Bucksch *et al.*, 2010).

Correctness of the branching hierarchy is a prerequisite to enable proper navigation through the tree structure, while centeredness enables us, e.g., to measure diameters and length of tree parts. The resulting skeleton graph produced by the skeletonization algorithm is shown in Figure 2d next to the point cloud it originated from.

Figure 2 also shows one of the major mathematical problems with laser scanned trees, the youngest branches are strongly under-sampled (Bucksch *et al.*, 2009a). Furthermore, at higher crown densities, the amount of occlusion effects is increased, leading to gaps in the point cloud because of insufficient coverage of the tree surface. A small incidence angle between the laser beam and the tree surface can lead to increased noise, because of the round surface geometry of the branches (Soudarissanane *et al.*, 2008). Increased noise may also be due to tie points being unevenly distributed in space (Fleck *et al.*, 2010b). The increased noise leads to the fact that some (especially smaller) branches may not be skeletonized. For details on this particular skeletonization algorithm, the reader is referred to Bucksch *et al.* (2009a) and Bucksch *et al.* (2010).

### Branch Length Estimation

The output of the skeletonization process is a graph (Figure 2d) consisting of vertices connected by edges centered within the tree. Estimation of branch length requires a graph-splitting procedure (Plate 1) to segment the skeleton graph into subgraphs representing a single branch. Three steps are involved to derive single branches from the skeleton graph:

1. Determination of the trunk base vertex; we have chosen the vertex with the smallest z-coordinate as the trunk base.
2. A tracing along the graph to follow the branch vector.
3. A criterion for deciding which edge belongs to the currently followed branch at branching vertices; the criterion used was based on the deviation from a 180° elongation of the branch axis; note that vertices with more than two incident edges represent the start of a new branch.

The skeleton graph allows navigation through the tree point cloud. At every vertex with more than two incident edges (marked red in Plate 1) the graph has to be split into

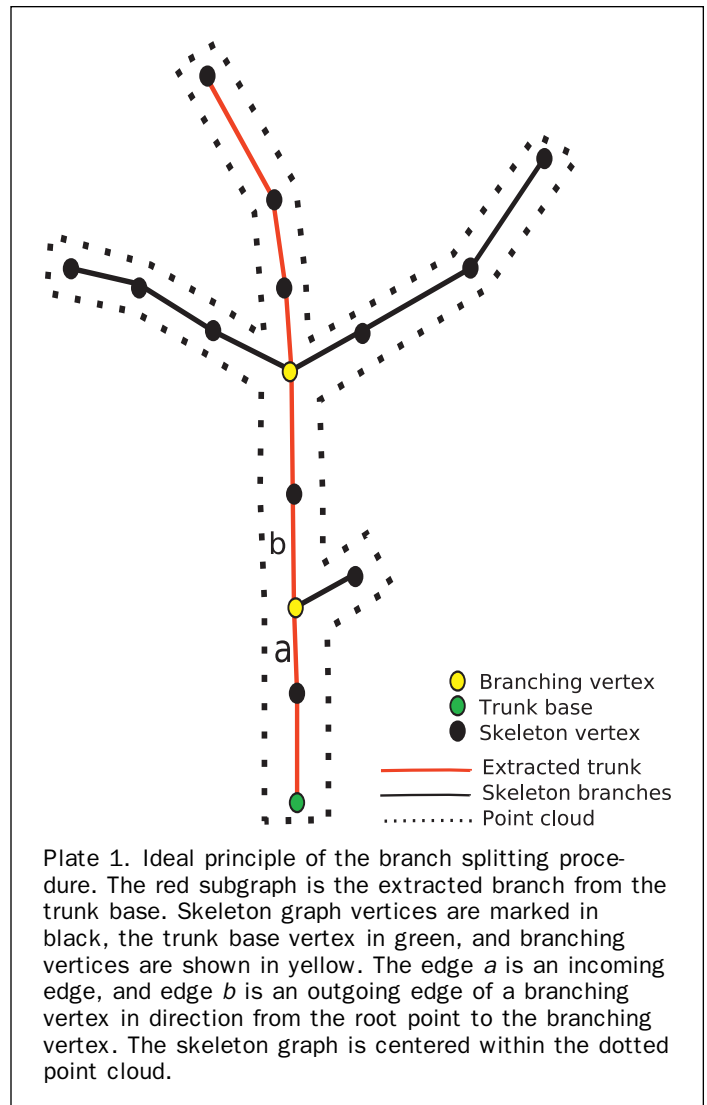


Plate 1. Ideal principle of the branch splitting procedure. The red subgraph is the extracted branch from the trunk base. Skeleton graph vertices are marked in black, the trunk base vertex in green, and branching vertices are shown in yellow. The edge 'a' is an incoming edge, and edge 'b' is an outgoing edge of a branching vertex in direction from the root point to the branching vertex. The skeleton graph is centered within the dotted point cloud.

the currently followed branch and newly starting branches. By tracing the graph from the trunk base, we can identify the edge 'a' (Plate 1) reaching a branching point. The incident edge 'b' forming the angle closest to 180 degree between 'a' and 'b' is selected to continue tracing (purple subgraph in Plate 1). All other incident edges are marked as branch bases from which a new trace can be started. This procedure also provides the branch hierarchy as an output. The skeleton graph is geometrically embedded into the tree point cloud and the Euclidean length of all edges in one trace is used as the branch length.

### Branch Diameter Estimation

The output of the branch length estimation is a segmentation of the tree in its branches. Every branch is represented as a graph containing either two vertices ( $v_1$  and  $v_2$ ) with one incident edge or several vertices between  $v_1$  and  $v_2$  with two incident edges. In other words, a branch is represented as a collection of line segments having no branching points.

One property of the SKELTRE-skeletonization procedure (Bucksch *et al.*, 2009a) is the relationship between every vertex in the skeleton graph to a set of points  $p_i$  in the point cloud. As the skeleton graph is assumed to be

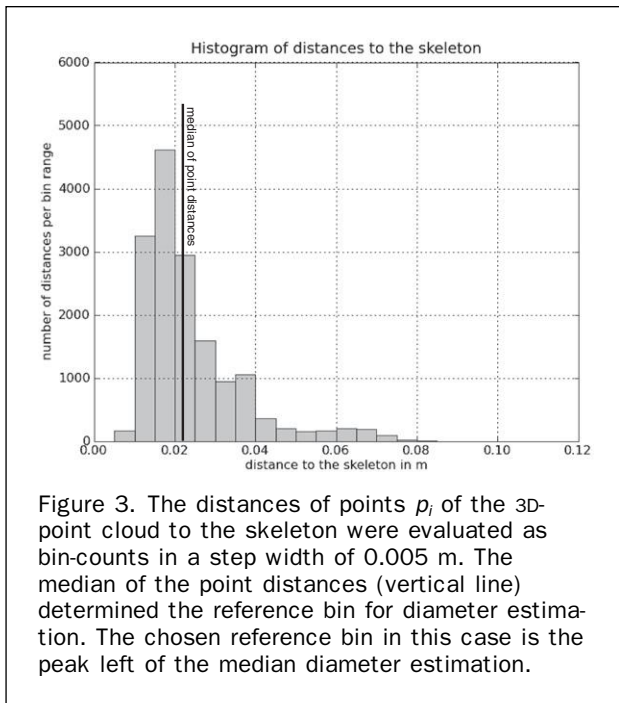


Figure 3. The distances of points  $p_i$  of the 3D-point cloud to the skeleton were evaluated as bin-counts in a step width of 0.005 m. The median of the point distances (vertical line) determined the reference bin for diameter estimation. The chosen reference bin in this case is the peak left of the median diameter estimation.

centered in the point cloud (Plate 1), the distances of all  $p_i$  to the skeleton represent the radius of the branch. Because a  $p_i$  corresponds to a vertex and not to an edge, we calculate the distances of all  $p_i$  to all incident edges of the corresponding vertex. Note that the maximum number of incident edges is two. The smallest distance to one of the edges was used for further processing. After calculating the distances of all  $p_i$ , a histogram was calculated with bin-size 0.005 m (Figure 3). Starting from the bin containing the median of all distances (vertical line in Figure 3), the peak closest to the median-bin was selected as a reference bin for the branch radius. The average value of this bin was taken as the radius of the branch. This method was adapted for terrestrial laser scan data from Bucksch *et al.* (2009b).

#### Data Preparation

The diameter measurements from the manual and automated methods were sorted in ascending order. This sorting enabled a one-to-one comparison of the measured values, because the manually-measured tree hierarchy differed from the one measured automatically. Furthermore, the manual measurement contained more measured branches than the automatic measurements, because branches smaller than 3 mm in diameter are not captured by the laser scanner, respectively, result in noise which is filtered out by the scanner software. As mentioned in Bucksch *et al.* (2009a), finer branches result in a single line due to individual points representing the entire width of a twig. This makes it impossible to extract a diameter from it. Due to this limitation, the smaller branches from the manual measurement were removed to assure two equally sized datasets. It should be stated that the length remained extractable because the length point data is represented independently from the diameter point data. This expected difference in the extractable diameter is also shown in Table 1. To compare the manual measurements to the automatic measurements, a linear regression was calculated for all six trees.

TABLE 1. COMPARISON OF THE OVERALL EXTRACTED LENGTH BETWEEN SKELETON AND FIELD MEASUREMENT AND THE OVERALL EXTRACTED LENGTH OF BRANCHES WHERE A DIAMETER COULD BE OBTAINED. THE RATIO IN THE LAST COLUMN IS THE RATIO BETWEEN COLUMN 1 AND COLUMN 3

Tree	Overall length of the skeleton	Overall length of the field data	Overall length of branches with extractable diameter and ratio
Apple 1	95.9 m	68.1 m	57.3 m (60%)
Apple 2	47.4 m	41.7 m	35.3 m (74%)
Apple 3	40.9 m	37.9	26.8 m (66%)
Apple 4	52.3 m	53.9	44.3 m (85%)
Apple 5	128.4 m	122.8	104.6 m (81%)
Apple 6	111.8 m	103.4	75.1 m (67%)

## Results and Discussion

### Skeletons

The algorithm showed good stability to gaps and robustness to noise in the point cloud (Figure 4). Where gaps in the measured data occur, the algorithm still detected the two parts of a branch on both sides of the gap. This resulted in the simulation of a higher number of branch segments than we measured by hand. Small artifacts were sometimes rendered at the trunk base due to parts of surrounding ground elements (grass, moss or soil) represented in the 3D-point cloud.

### Branch Length

Digitally rendered branch lengths were compared to the hand measurements based on frequency distributions of the total amount of branches of a tree. The branch length was categorized in length classes of 5 cm from 0 to maximum occurring branch length of each tree. The results for the six apple trees demonstrating this categorization are shown in Figures 5 and 6. While the algorithm detected a much higher number of small segments (classes up to 5 cm and up to 10 cm) and did recognize a few longer branches that were measured as separate entities in the hand measurements, the pattern in the middle classes between 20 cm and 65 cm was usually well correlated between both methods (Figure 5 and Figure 6).

The correlation between the automatically detected branch-length classes of all apple trees except the lowest two classes and their associated hand-measured branch-length classes yielded an  $r^2$  of 0.48 (Plate 2). A regression line showed that the branch number in hand-measured branch-length classes was on average 49.3 percent of the branch number in the associated branch-length class of the automatically detected branches. Since this percentage did not substantially vary over branch-length classes, all branch-length classes appeared to be similarly affected by gaps in the 3D-laserscanner data. The overall length of the skeleton and the manually measured length in the field differed not substantially except for Apple 1. The point cloud of Apple 1 contains some parts of the trellis system, which could not be filtered out and count therefore to the overall skeleton length. On average, the field measured length deviated 7.2 percent from the automatically extracted length for all trees except Apple 1. Remember here, that the chosen trees are orchard trees containing a high proportion of branches with diameter smaller than 1 cm, unlike bigger trees in a forest, where longer and wider branches occur. These observations are also reflected in Table 2.

The described analysis procedure was applied to six apple trees as shown in Table 1. It can be seen that the

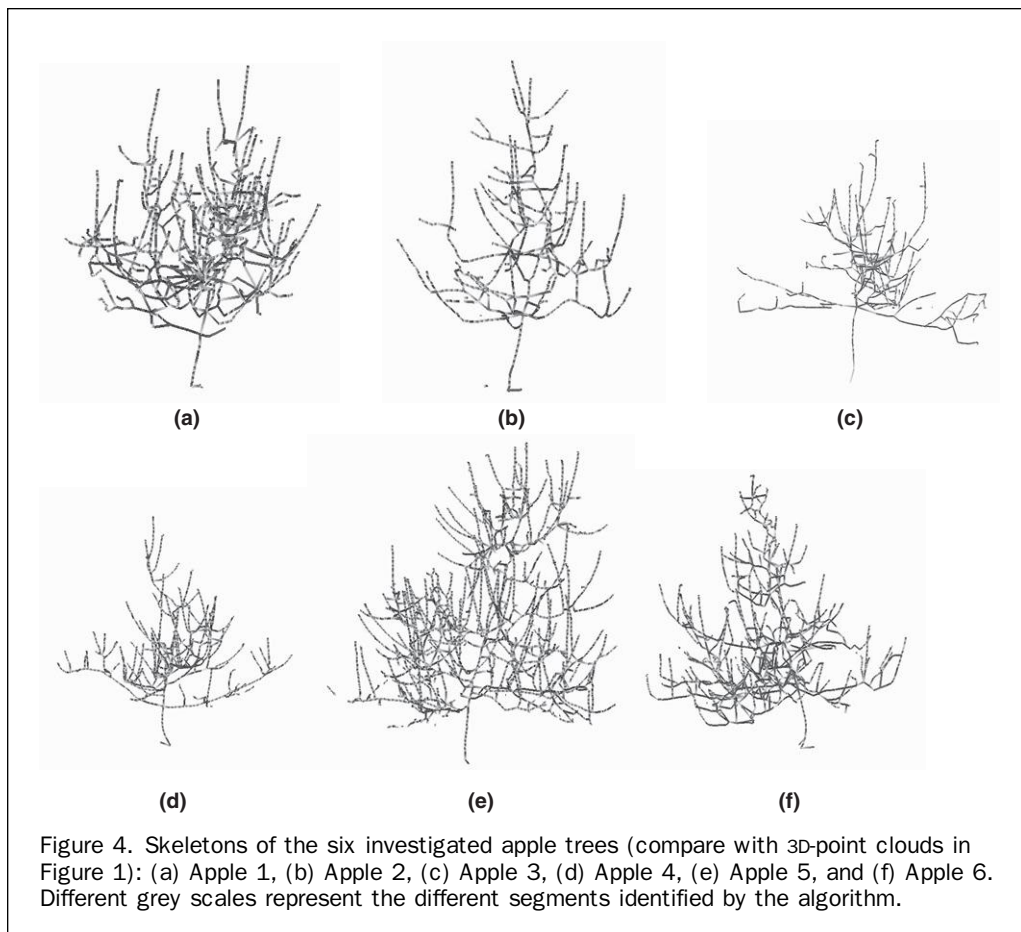


Figure 4. Skeletons of the six investigated apple trees (compare with 3D-point clouds in Figure 1): (a) Apple 1, (b) Apple 2, (c) Apple 3, (d) Apple 4, (e) Apple 5, and (f) Apple 6. Different grey scales represent the different segments identified by the algorithm.

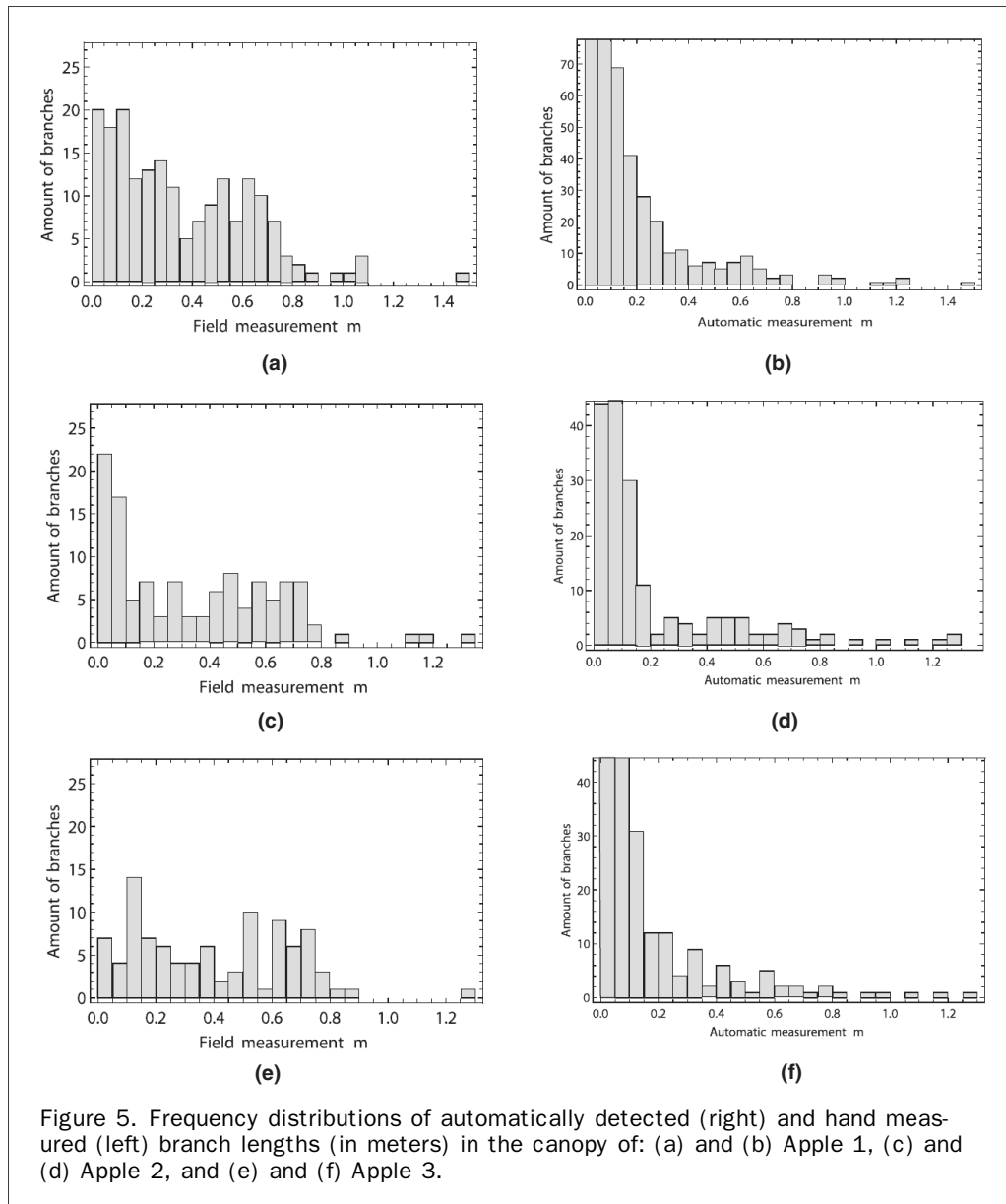
result is not heavily dependent on the crown complexity. As an indicator of crown complexity, the trunk diameter is given in Table 2.

#### Branch Diameter

For the six candidate trees the frequency distributions of field and automatic diameter measurement were calculated, as shown in Figure 7 and Figure 8. A high similarity of the histogram shape could be observed and assessed by linear regression (Table 2). A Chi-squared test to evaluate the good results of the histograms showed that there is no significant difference between the frequency distributions of field and the automatic measurements. For all trees correlation coefficients above 0.9 for the diameter could be achieved (Table 2). We expected a greater influence of the edge effect on the finer branches, which was already observed by Lichti *et al.* (2002) and Boehler *et al.* (2003).

A larger difference between the skeleton measurement and the manual measurement can be observed at the largest value representing the trunk. Two aspects explain this behavior. First, the field measurements were made with a measuring tape, which measures the convex hull of the rough trunk (the trunk outside the bark), while the automatic procedure measures the smallest distance to the skeleton of the data points obtained from the hull and selects a suitable bin close to the diameter. Second, the field measurement relies on the main vertical axis of the tree, which does not reflect possible curvatures of the trunk. This difference could be assessed by an alternative test measurement with the Cyclone software (Leica Geosystems). Cylinders were fitted into several slices along the

trunk using a standard least squares fitting method. We noticed differences from the manual field measurements of up to 2 cm due to bulges not considered in the manual measurement. These results are comparable to the results found in Henning and Radtke (2006), who evaluated the measurement error of trunk cross sections in a forest using a terrestrial laser scanner. They observed errors in the order of 1 cm to 2 cm. The smaller branch sizes of the studied orchard trees demand a different method for diameter estimation, because of increased noise due to the edge effect. The better correlations found for the tree diameter compared to the length measurements is explained by the differences induced by different branch segmentation between field measurement and automatic measurement, which is also the main reason for the generally higher number of branches in the automatic diameter detection compared to the field measurements. The results here show that the frequency distribution of diameters is robust to branch hierarchy errors resulting from branch segmentation process. In Plate 3 the scatter plot of all diameters at all automatically and manual measured diameters are shown. The scatter plot assumes that all diameters are extracted in one-one correspondence of field and automatic measurement. Therefore the diameters of the field measurements were matched to the closest automatic measurement and shows a qualitative measure of the diameter estimation in the color coding. The coloring of the scatter plot gives a qualitative measure for the number of points used to calculate the diameter in the selected histogram bin. The coloring reflects the normalized amount of points with respect to the maximal



amount used for a diameter calculation. If a one-to-one correspondence of the diameters is assumed, the overall regression is given as 0.98 and the  $p$ -value of 0.0 indicates that the field measurement fully correlates with the automatic measurement. Note that this assumption is based on the good correlation results of the frequency distributions. The observable grouping behavior emerges from the histogram binning used to estimate the diameter. The calculations were done with the SciPy package in Python.

## Conclusions

This paper presents a new approach for extracting the branching architecture from leafless apple trees. This approach is based on a skeleton extraction procedure based on terrestrial laser scan data. On selected examples we showed that high correlation between manual validation measurements and automatically extracted branch length detection is achievable, although problems with

gaps in the 3D-laserscanner data were obvious. The frequency distributions of the length estimations for lengths above 5 cm correlated with coefficients of 0.41 to 0.78, while the diameters, where the effect of gaps does not directly influence the correlation, showed much better correlations.

The frequency distributions of the diameter estimations show a high similarity in their shape for diameters bigger than 0.5 cm. The shape similarity between the frequency distributions of field data and automatic measurements was assessed by a linear regression. The correlation coefficients of all six trees are above 0.9, and show that the branch segmentation has no bigger influence on the diameter distributions.

The more complex the canopy structure of trees, the more gaps are to be expected in the scanned data, a problem which remains to be solved in the algorithmic calculation. Skeletonization algorithms such as the proposed SKELTRE method provide a basis for an adequate gap-filling strategy in 3D-point clouds with a high degree of occlusion.

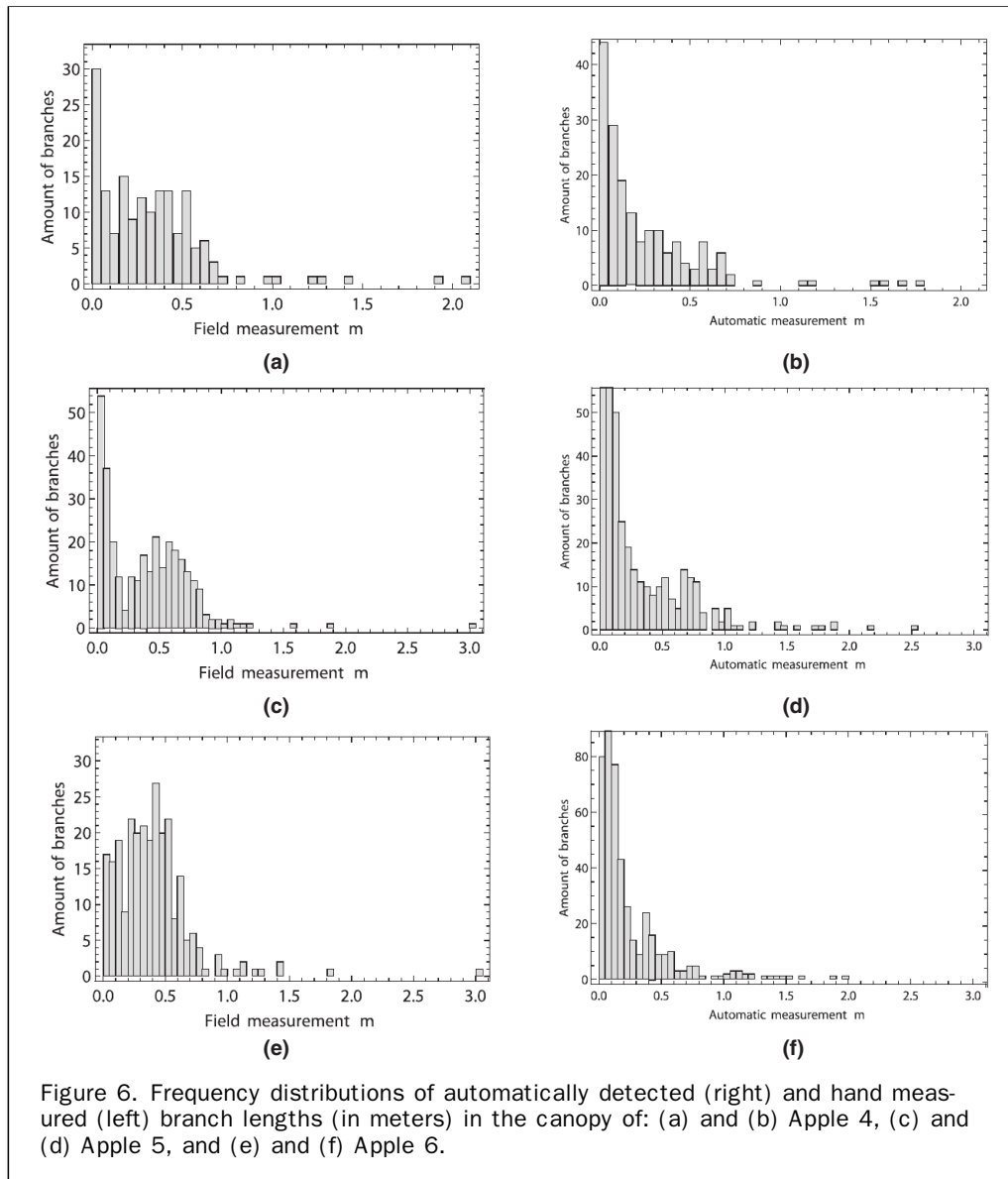


Figure 6. Frequency distributions of automatically detected (right) and hand measured (left) branch lengths (in meters) in the canopy of: (a) and (b) Apple 4, (c) and (d) Apple 5, and (e) and (f) Apple 6.

TABLE 2. RESULTS OF THE CANOPY ANALYSIS OF SIX VALIDATION TREES. THE CROWN COMPLEXITY IS INDICATED BY THE STEM DIAMETER. THE SIMILARITY OF THE FREQUENCY DISTRIBUTIONS IS GIVEN AS THE CORRELATION COEFFICIENT BETWEEN THE FIELD DATA AND THE AUTOMATIC DATA

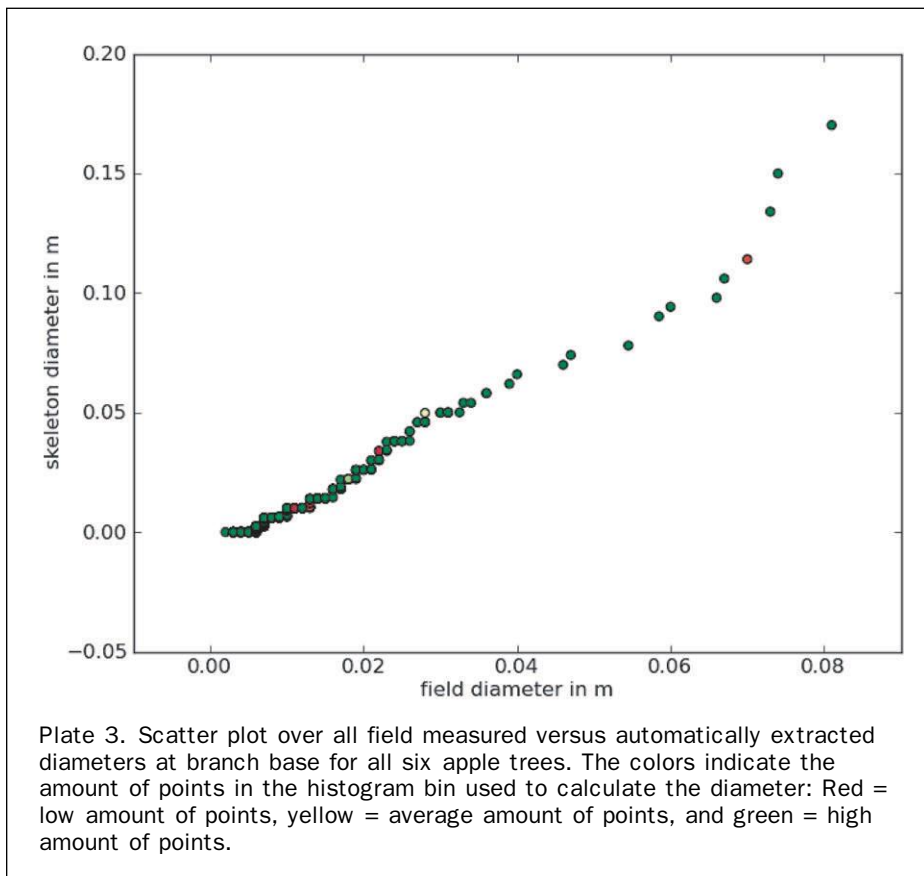
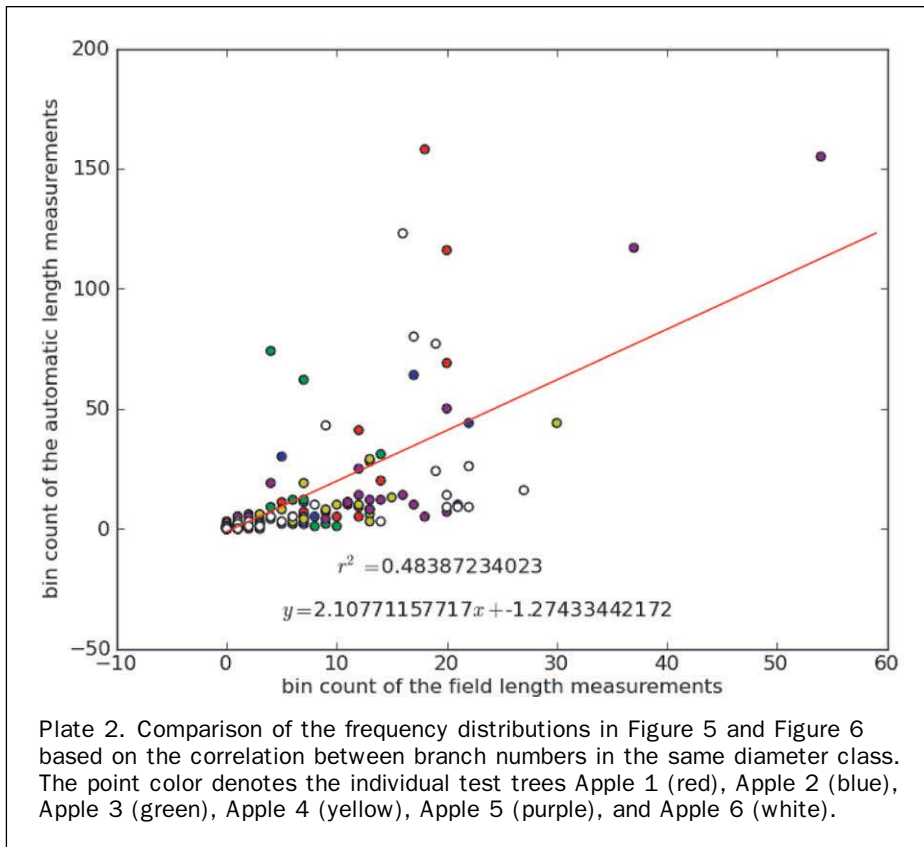
Tree	Diameter of trunk	R <sup>2</sup> Length	R <sup>2</sup> Diameter
Apple 1	7.3 cm	0.78	0.92
Apple 2	6.7 cm	0.41	0.95
Apple 3	3.9 cm	0.64	0.98
Apple 4	5.9 cm	0.77	0.99
Apple 5	8.1 cm	0.72	0.98
Apple 6	7.4 cm	0.62	0.99

The overall length of the extracted skeleton and the field measurement varied by only 7.5 percent. A diameter could be obtained for 72 percent of the overall skeleton length. The loss of extractable diameters compared to the extracted skeleton length is reasoned in the strong under-sampling of the finer branches.

Further work will focus on the evaluation of the extractable biomass based on the frequency distributions. For this reason, we expect to improve the correlation of the branch length by incorporating the diameter into the graph-splitting procedure. It is expected that the use of a diameter criterion will fully reveal the branching hierarchy under the assumption that a new branch is always thinner than the branch from which it is originating from. The approximation of the field measurement procedure will enable better simulation of individual branches, which is useful on trees with a small number of branches available for regression analysis. Most notably, the entire extraction process of branch length and diameters was carried out without the use of allometric relationships. The use of this method for light-driven modeling of physiological tree parameters, e.g., branch transpiration will be assessed by investigating the representation of the branch locations of the skeleton

### Acknowledgments

We want to thank Lyle Almond and all the reviewers for their valuable comments.



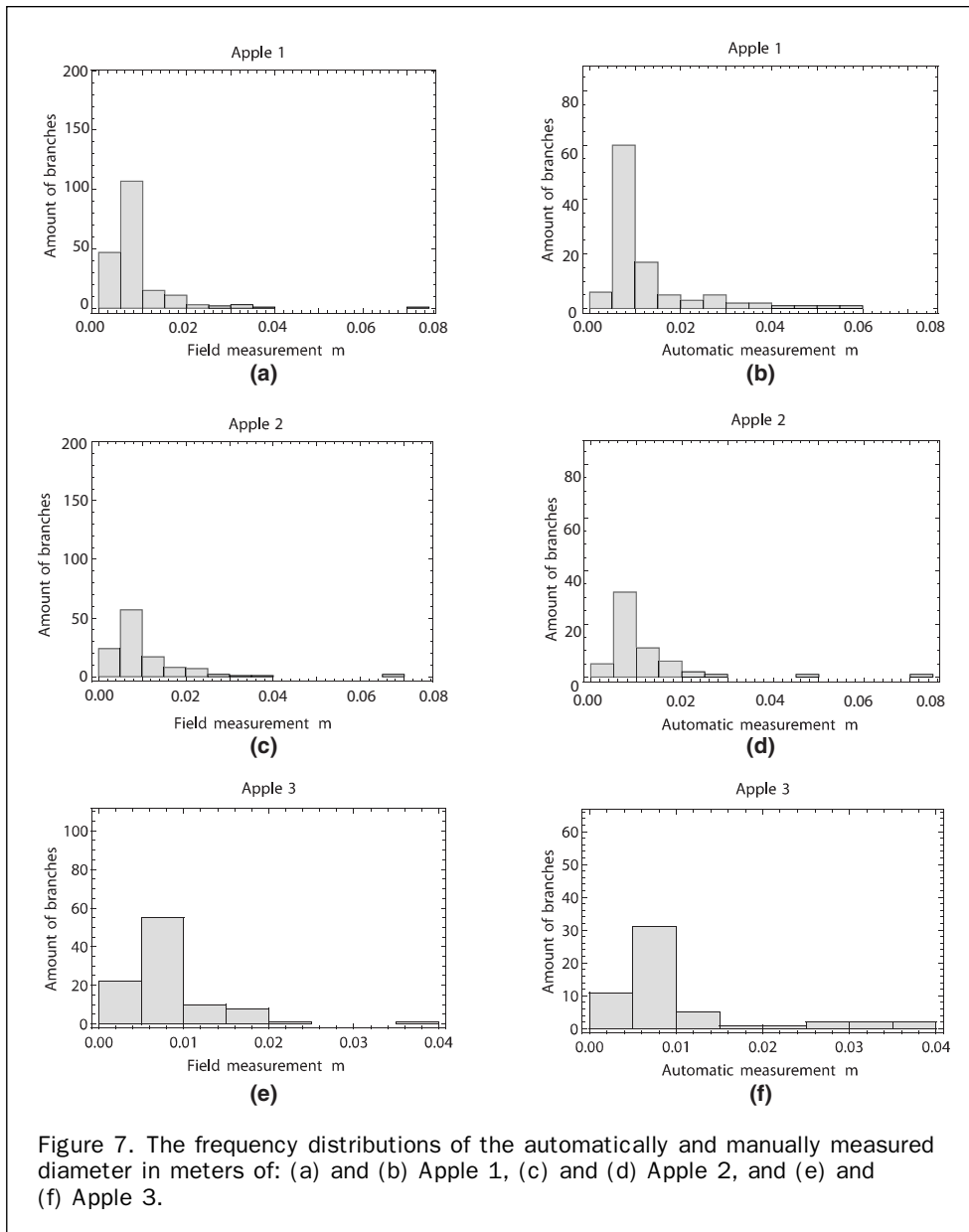


Figure 7. The frequency distributions of the automatically and manually measured diameter in meters of: (a) and (b) Apple 1, (c) and (d) Apple 2, and (e) and (f) Apple 3.

## References

- Bartelink, H.H., 1997. Allometric relationships for biomass and leaf area of beech (*Fagus sylvatica* L), *Annales de Science Forestiere*, 54:39-50
- Biasotti, S.A., D. Boissonnat, J.-D. Edelsbrunner, H. Elber, G. Mortara, M. Sanniti di Baja, G. Spagnuolo, M. Michela Tanase, and R. Veltkamp, 2008. Skeletal Structures. Chapter 6 *Shape Analysis and Structuring* (L. De Floriani and M. Spagnuolo, editors), Springer.
- Boehler, W., and A. Marbs, 2003. Investigating Laser Scanner Accuracy, *Proceedings of the CIPA Symposium 2003*.
- Bucksch, A., R. Lindenbergh, and M. Menenti, 2010. SkelTre - Robust skeleton extraction from imperfect point clouds, *The Visual Computer*, Springer, DOI: 10.1007/s00371-010-0520-4.
- Bucksch, A., R. Lindenbergh, and M. Menenti, 2009a. SkelTre - Fast skeletonization of imperfect point clouds of botanic trees, *Proceedings of Eurographics/ACM Siggraph Symposium on 3D Object Retrieval*, 28 March to 03 April, Munchen.
- Bucksch, A., R. Lindenbergh, M. Menenti, and M.Z. Raman, 2009b. Skeleton-based botanic tree diameter estimation from dense LiDAR data, *Proceedings of SPIE*, SPIE, Bellingham, Washington, Vol. 7460.
- Bucksch, A., and R. Lindenbergh, 2008. CAMPINO - A skeletonization method for point cloud Processing, *ISPRS Journal of Photogrammetry and Remote Sensing*, 63(1):115-127.
- Burger, H. 1945. Holz, Blattmenge und Zuwachs - Die Buche, *Mitteilungen der Schweizerischen Anstalt für das Forstliche Versuchswesen*, 26:419-468
- Fleck, S. 2002. *Integrated Analysis of Relationships between 3D-structure, Leaf Photosynthesis, and Branch Transpiration of Mature Fagus sylvatica and Quercus petraea Trees in a Mixed Forest Stand*, Ph.D. Thesis, Bayreuther Forum Ökologie Nr. 97, 183 p.
- Fleck, S., D. van der Zande, M. Schmidt, and P. Coppin, 2004. Reconstructions of tree structure from laser-scans and their use to predict physiological properties and processes in canopies, *International Archives of the Photogrammetry, Remote Sensing and Spatial Information Sciences*, 36(8/W2):119-123.
- Fleck, S., N. Obertreiber, I. Schmidt, M. Brauns, H. Jungkunst, and C. Leuschner, 2007. Terrestrial lidar measurements for analysing

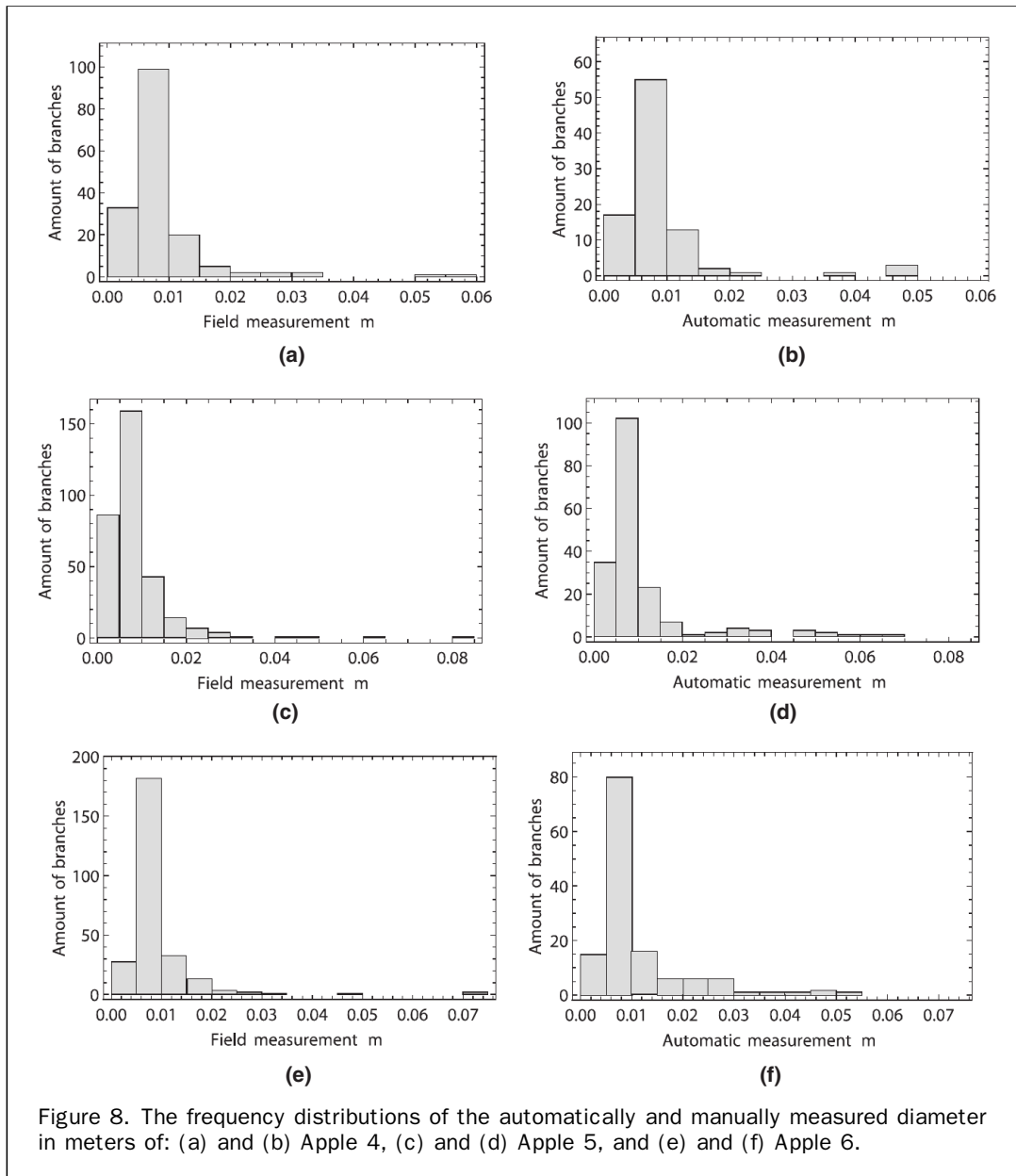


Figure 8. The frequency distributions of the automatically and manually measured diameter in meters of: (a) and (b) Apple 4, (c) and (d) Apple 5, and (e) and (f) Apple 6.

canopy structure in an old-growth forest, *International Archives of the Photogrammetry, Remote Sensing and Spatial Information Sciences*, 26(3/W52):125-129

Fleck, S., C.G. Embree, and D. Nichols, 2010a. The systematic influence of Crop Load, Spur Type, 3D-Canopy Structure, and Leaf Zonal Chlorosis on leaf photosynthesis of 'Honeycrisp' Apple Trees, *Acta Horticulturae*, (accepted 2009)

Fleck, S., I. Mölder, M. Jacob, H. Jungkunst, T. Gebauer, and C. Leuschner, 2010b. Comparison of conventional 8-point crown projections with lidar-based virtual crown projections in a temperate old-growth forest, *Annals of Forest Science*, (submitted)

Gorte, B., and N. Pfeifer, 2004. Structuring laser-scanned trees using 3D mathematical Morphology, *International Archives of Photogrammetry and Remote Sensing*, Vol. XXXV, B5, pp. 929-933

Gorte, B., 2006. Skeletonization of laser-scanned trees in the 3D raster domain, *Lecture Notes in Geoinformation and Cartography: Innovations in 3D Geo Information Systems*, Berlin Heidelberg: Springer, pp. 371-381.

Henning, J.G., and P.J. Radtke, 2008. Multiview range-image registration for forested scenes using explicitly-matched tie points estimated from natural surfaces, *ISPRS Journal of Photogrammetry and Remote Sensing*, 63(1):68-83.

Henning, J.G., and P.J. Radtke, 2006. Detailed stem measurements of standing trees from ground-based scanning LiDAR, *Forest Science*, 52:67-80.

Lichti, D.D., S.J. Gordon, M.P. Stewart, J. Franke, and M. Tsakiri, 2002. Comparison of digital photogrammetry and laser scanning, *Proceedings of the CIPA WG6 International Workshop on Scanning for Cultural Heritage Recording*.

Niklas, K.J., 1994. *Plant Allometry: The Scaling of Form and Process*, The University of Chicago Press, Chicago-London.

Palágyi, K., E. Sorantin, E. Balogh, A. Kuba, C. Halmaj, B. Erdőhelyi, and K. Hausegger, 2001. A sequential 3D thinning algorithm and its medical applications, *Proceedings of the 17<sup>th</sup> International Conference on Information Processing in Medical Imaging*, IPMI Davis, California, *Lecture Notes in Computer Science*, Springer.

Pfeifer, N., B. Gorte, and D. Winterhalder, 2004. Automatic reconstruction of single trees from terrestrial laser scanner data, *Proceedings of 20<sup>th</sup> ISPRS Congress*, Istanbul, Turkey.

Roloff, A. 1986. *Morphologie der Kronenentwicklung von Fagus sylvatica L. (Rotbuche) Unter Besonderer Berücksichtigung Möglicherweise Neuartiger Veränderungen*, Ph.D. Dissertation, Universitaet Goettingen.

Serra, J. 1982. *Image Analysis and Mathematical Morphology*, Academic Press, London.

Shan, J., and C. Toth (editors), 2008. *Topographic Laser Ranging and Scanning*, CRC Press.

Soudarissanane, S., R. Lindenbergh, and B. Gorte, 2008. Reducing the error in terrestrial laser scanning by optimizing the measurement set-up, *Proceedings of the 21<sup>st</sup> ISPRS Congress*, Beijing, China.

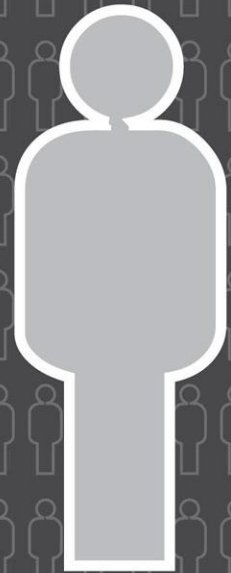
Xu, H.G., and C.B. Nathan, 2007. Knowledge and heuristic-based modelling of laser-scanned Trees, *ACM Transactions on Graphics (TOG)*, Vol. 26, Nr. 4.

Yan, D.M., J. Wintz, B. Mourrain, W. Wang, F. Boudon, and C. Godin, 2009. Efficient and robust branch model reconstruction from laser scanned points, *Proceedings of the 11<sup>th</sup> IEEE International Conference on Computer-Aided Design and Computer Graphics*.

# Stand out from the rest— earn ASPRS Certification

*"ASPRS Certification is a highly sought after credential by employers and clients. Since receiving my certification, I find I get more respect from my peers and clients."*

**Raquel Charrois, Certified Photogrammetrist 1240**



**Apply now for one of these ASPRS Certifications:**

- **Photogrammetrist**
- **Mapping Scientist - Remote Sensing**
- **Mapping Scientist - GIS/LIS**
- **Photogrammetric Technologist**
- **Remote Sensing Technologist**
- **GIS/LIS Technologist**